

Status of the two-Higgs-doublet model of type II

Otto Eberhardt,^a Ulrich Nierste,^a and Martin Wiebusch^a

^a*Institut für Theoretische Teilchenphysik, Karlsruhe Institute of Technology, Engesserstraße 7, 76128 Karlsruhe, Germany*

E-mail: otto.eberhardt@kit.edu, ulrich.nierste@kit.edu,
martin.wiebusch@kit.edu

ABSTRACT: We determine the allowed parameter space of the CP -conserving two-Higgs-doublet model (2HDM) of type II with a softly broken Z_2 symmetry. Our analysis includes theoretical constraints from vacuum stability and perturbativity as well as experimental constraints from signal strengths of the 126 GeV Higgs boson, the non-observation of additional Higgs resonances and electroweak precision and flavour observables. If the 126 GeV resonance is interpreted as the light CP -even Higgs boson of the 2HDM our analysis shows that scenarios where the couplings of this boson deviate substantially from those of the SM Higgs boson are disfavoured at one standard deviation and completely excluded for small values of $\tan\beta$. We also discuss bounds on the masses of the heavy 2HDM Higgs bosons and their implications for the possible decay modes of these particles. We find that the region in which both non-standard neutral Higgs bosons are simultaneously lighter than 300 GeV is excluded at two standard deviations.

Contents

1	Introduction	1
2	The Model	2
3	Theoretical Constraints and Experimental Inputs	3
4	Results	7
5	Conclusions	10

1 Introduction

The LHC experiments ATLAS and CMS have discovered a neutral boson whose properties comply with those of the Standard-Model (SM) Higgs boson [1, 2]. Moreover, the data on the Higgs signal strength have permitted to exclude a sequential fourth fermion generation at the level of 5 standard deviations [3–8]. Similarly to the number of fermion generations, the structure of the Higgs sector is an ad-hoc feature of the SM: While a single Higgs doublet is sufficient to break the electroweak symmetry, there are no fundamental reasons forbidding a richer Higgs sector. From a purely phenomenological point of view, the logical next step after the discovery of a Higgs boson is to address the question whether it really is “the” Higgs boson. If nature has opted for an extended Higgs sector, the latter will influence precision observables through loops with extra Higgs bosons. In order to assess the viable parameter space of a given extension of the SM, one must perform a global fit in the extended model which includes all relevant theoretical and experimental constraints. In this paper we perform such an analysis for the popular two-Higgs-doublet model (2HDM) [9] of type II [10, 11], in the widely-studied version without CP violation in the Higgs potential.

The presence of an additional Higgs doublet implies the existence of three neutral (h , H , A) and two charged (H^\pm) Higgs bosons. The 2HDM of type-II is designed to avoid flavour-changing couplings of the neutral Higgs boson by coupling one Higgs doublet solely to up-type and the other one to down-type fermions. Theoretical constraints on this model come from the following requirements:

- the Higgs potential must be bounded from below,
- neglecting the possibility of a meta-stable vacuum, the minimum of the Higgs potential with a vacuum expectation value (VEV) $v = 246$ GeV must be the global minimum,
- the Higgs and Yukawa couplings must be perturbative.

The relevant experimental constraints are:

- the mass and signal strengths of the observed Higgs resonance at 126 GeV,
- the non-observation of additional Higgs resonances at LEP, Tevatron and the LHC,
- the electroweak precision observables measured at LEP,
- flavour observables from radiative B decays and $B - \bar{B}$ mixing.

A comprehensive and thorough analysis of constraints from flavour physics has been performed by the CKMfitter group in [12]. In our study we only include the two most relevant flavour observables, namely the branching ratio of $\bar{B} \rightarrow X_s \gamma$ and the $B_s - \bar{B}_s$ mixing frequency. After the Higgs discovery the compatibility of the type-II 2HDM with the observed Higgs signal strengths and other experimental data has been studied in several papers [13–22]. However, to our knowledge the analysis presented here is the first global fit which consistently includes all the above-mentioned constraints. The Higgs signal strengths provide strong bounds on the 2HDM parameters which determine the couplings of the light CP -even Higgs h , namely on the ratio $\tan \beta$ of the Higgs VEVs and the mixing angle α of the neutral CP -even Higgs bosons. In this respect, our analysis updates (some of the) previous studies by using the Higgs data presented at the Moriond 2013 conference. Furthermore, the above-mentioned theoretical and experimental constraints allow us to rule out certain combinations of the heavy 2HDM Higgs masses. We also discuss the implications of these limits for the possible decay modes of heavy 2HDM Higgs bosons. Where appropriate, we compare our results with those of [13–22].

Our paper is organised as follows: in Sec. 2 we provide a brief overview over the type-II 2HDM and its parametrisation. In Sec. 3 we discuss the theoretical and experimental constraints included in our analysis in detail. The results of the global fit are shown in Sec. 4.

2 The Model

The model we consider in this paper is the CP -conserving two Higgs doublet model of type II with a softly broken Z_2 symmetry. All relevant details about this model can be found in [23], whose notational conventions we follow exactly. The Higgs potential we consider is

$$\begin{aligned}
 V = & m_{11}^2 \Phi_1^\dagger \Phi_1 + m_{22}^2 \Phi_2^\dagger \Phi_2 - m_{12}^2 (\Phi_1^\dagger \Phi_2 + \Phi_2^\dagger \Phi_1) + \frac{1}{2} \lambda_1 (\Phi_1^\dagger \Phi_1)^2 + \frac{1}{2} \lambda_2 (\Phi_2^\dagger \Phi_2)^2 \\
 & + \lambda_3 (\Phi_1^\dagger \Phi_1) (\Phi_2^\dagger \Phi_2) + \lambda_4 (\Phi_1^\dagger \Phi_2) (\Phi_2^\dagger \Phi_1) + \frac{1}{2} \lambda_5 [(\Phi_1^\dagger \Phi_2)^2 + (\Phi_2^\dagger \Phi_1)^2] \quad , \quad (2.1)
 \end{aligned}$$

where Φ_1, Φ_2 are the two scalar $SU(2)$ doublets. Under the Z_2 symmetry they transform as $(\Phi_1, \Phi_2) \rightarrow (-\Phi_1, \Phi_2)$ and the term with m_{12}^2 breaks that symmetry softly. In this paper we only study the case of unbroken CP symmetry (in the Higgs sector), where we can assume without loss of generality that $m_{11}^2, m_{22}^2, m_{12}^2, \lambda_1, \dots, \lambda_5 \in \mathbb{R}$. At the global minimum of the potential V the neutral components of Φ_1 and Φ_2 acquire vacuum expectation values (VEVs) $v_1/\sqrt{2}$ and $v_2/\sqrt{2}$, respectively, which are determined by the parameters of the

	WW, ZZ	up-type quarks	down-type quarks, leptons
h	$\sin(\beta - \alpha)$	$\cos \alpha / \sin \beta$	$-\sin \alpha / \cos \beta$
H	$\cos(\beta - \alpha)$	$\sin \alpha / \sin \beta$	$\cos \alpha / \cos \beta$
A	0	$\cot \beta$	$\tan \beta$

Table 1: Tree-level couplings of the neutral 2HDM Higgs bosons to gauge bosons and fermions. Each coupling is normalised to the corresponding coupling of the SM Higgs boson.

Higgs potential and must satisfy $v_1^2 + v_2^2 = (246 \text{ GeV})^2 \equiv v^2$. After trading m_{11} and m_{22} for v_1 and v_2 the independent real parameters of the model are

$$\tan \beta = v_2/v_1 \quad , \quad m_{12}^2 \quad , \quad \lambda_1 \quad , \quad \lambda_2 \quad , \quad \lambda_3 \quad , \quad \lambda_4 \quad , \quad \lambda_5 \quad (2.2)$$

and we may assume $\tan \beta > 0$ without loss of generality. The physical scalar spectrum of this model consists of two neutral CP -even bosons h and H (with masses $m_h \leq m_H$), a neutral CP -odd boson A , a charged boson H^+ and its anti-particle H^- . Expressions for the physical (tree-level) masses of the Higgs bosons in terms of the parameters (2.2) can be found in [23].

The Yukawa Lagrangian of the type-II model is

$$\mathcal{L}_{\text{Yuk}} = -Y_{ij}^d \bar{Q}_{Li} \Phi_1 d_{Rj} - Y_{ij}^u \bar{Q}_{Li} \tilde{\Phi}_2 u_{Rj} - Y_{ij}^l \bar{L}_{Li} \Phi_1 e_{Rj} + \text{h.c.} \quad , \quad (2.3)$$

where Q_L and L_L are the left-handed quark and lepton doublets, d_R , u_R and e_R are the right-handed up-type quark, down-type quark and lepton singlets, respectively, Y^u , Y^d and Y^l are the corresponding Yukawa coupling matrices, $i, j = 1, 2, 3$ are generation indices and $\tilde{\Phi}_2 \equiv i\sigma_2 \Phi_2^*$ (where σ_2 is the second Pauli-Matrix).

The tree level couplings of the neutral CP -even Higgs bosons h , H to gauge bosons and fermions have the same structure as the corresponding couplings of the SM Higgs boson. The pseudo-scalar A only couples to fermions and the Feynman rule contains an additional factor $i\gamma_5$. The ratios of coupling constants (2HDM coupling divided by corresponding SM coupling) only depend on β and the mixing angle α of the neutral CP -even 2HDM Higgs bosons. These ratios are summarised in Table 1. The relation between α and the parameters (2.2) is given in [23]. For the discussion in this paper it is important to note that the couplings of the light CP -even Higgs h (first line of Table 1) approach the corresponding SM values for $\beta - \alpha \rightarrow \pi/2$, irrespective of the value of β .

3 Theoretical Constraints and Experimental Inputs

The parameters (2.2) are subject to a number of theoretical constraints. First of all, the potential (2.1) must be bounded from below. As explained in [23], this is the case if and only if the following inequalities are satisfied:

$$\lambda_1 > 0 \quad , \quad \lambda_2 > 0 \quad , \quad \lambda_3 > -\sqrt{\lambda_1 \lambda_2} \quad , \quad |\lambda_5| < \lambda_3 + \lambda_4 + \sqrt{\lambda_1 \lambda_2} \quad . \quad (3.1)$$

Furthermore, to obtain a stable vacuum state we require that the minimum of the potential with $v_1^2 + v_2^2 = (246 \text{ GeV})^2$ is the global minimum.¹ As pointed out recently in [24] this requirement leads to the additional constraint

$$m_{12}^2 (m_{11} - m_{22} \sqrt{\lambda_1/\lambda_2}) (\tan \beta - (\lambda_1/\lambda_2)^{1/4}) > 0 \quad . \quad (3.2)$$

Finally, if we want to be able to trust perturbative calculations, the magnitude of the Higgs self-couplings λ_i should not be too large. The only correct way to implement this bound is to compute many higher-order corrections and assess the convergence of the perturbative series. Here we take the simple approach of requiring $|\lambda_i| < \lambda_{\text{max}}$ for $i = 1, \dots, 5$ and some $\lambda_{\text{max}} > 0$. The most conservative choice for λ_{max} is 4π , which forces the product of two λ s and the loop factor to be smaller than 1. A study of higher-order corrections for the case of the SM Higgs sector points to a smaller perturbativity limit, closer to $\lambda_{\text{max}} = 2\pi$ [25]. To estimate the dependence of our results on the ultimately arbitrary upper limit λ_{max} we show results for $\lambda_{\text{max}} = 2\pi$ and $\lambda_{\text{max}} = 4\pi$.

In addition to these theoretical constraints, we confront the 2HDM described in Sec. 2 with the following experimental data:

- the mass of the observed Higgs resonance

$$m_h = 125.96_{-0.19}^{+0.18} \text{ GeV} \quad . \quad (3.3)$$

This input is a combination of the results presented in [26–29]. We always identify the observed Higgs resonance with the light CP -even 2HDM Higgs boson. Specifically, we neglect the possibility that the observed resonance is one of the heavy neutral 2HDM Higgs bosons or a degenerate state. See, for instance, [30, 31] for a discussion of the former case and [32] for the latter.

- the signal strengths (observed cross section times branching ratio divided by SM expectation) of the Higgs resonance at 126 GeV. Our signal strength inputs for the different decay modes and, in the case of the $\gamma\gamma$ final state, the different event categories defined by the experimental groups are summarised in Fig. 3. On the theory side, the signal strength for a given Higgs production and decay mode is given by the product of the corresponding 2HDM/SM ratios of (effective) squared couplings. For instance, the gluon fusion contribution $\mu(gg \rightarrow H \rightarrow \gamma\gamma)$ to the $H \rightarrow \gamma\gamma$ signal strength is given by the product $R_{gg}R_{\gamma\gamma}$, where R_{gg} ($R_{\gamma\gamma}$) is the square of the effective Hgg ($H\gamma\gamma$) coupling calculated in the 2HDM, divided by the same effective coupling calculated in the SM. We use the FeynArts, FormCalc and LoopTools packages [33–35] to compute R_{gg} and $R_{\gamma\gamma}$ at one-loop order. For all other couplings (HWW , HZZ etc.) we use the tree-level values.

To compare quantities such as $\mu(gg \rightarrow H \rightarrow \gamma\gamma)$ with experimental data one needs to know the composition of the Higgs signal in a given final state or event category.

¹In doing this we neglect the possibility that our vacuum is metastable with a lifetime larger than the age of the universe.

In other words, one needs to know the fraction with which each Higgs production mechanism contributes to the signal seen in each final state or event category. In our analysis we use these percentage contributions wherever they (or the corresponding selection efficiencies) are provided by the experimental groups. Our values for the percentage corrections are summarised in Tab. 3. In the case of the 8 TeV CMS $H \rightarrow \tau\tau$ data, we derived the percentage contributions from the corresponding selection efficiencies. These efficiencies are summarised in Tab. 2. For the remaining final states we assume that the dominant production mode contributes 100% of the signal.

- limits from searches for heavy neutral Higgs bosons in the WW and ZZ decay modes. Specifically, we include the (mass dependent) expected limit from the CMS $H \rightarrow WW \rightarrow 2l2\nu$ search ([36], Fig. 9) and the expected limit from the CMS $H \rightarrow ZZ \rightarrow 4l$ search ([29], Fig. 5, left panel). In the absence of any clear signals for heavy Higgs resonances we consider it good practice to use the expected limits instead of the observed ones since otherwise the analysis becomes sensitive to background fluctuations in the search data. For the same reason we refrain from using the signal strength values for heavy Higgs bosons, as provided by the experimental groups.
- the full set of electroweak pseudo-observables (EWPOs) measured at LEP and SLC, as well as the latest results for the W and top mass. We use the same inputs as in Table II of [8], and our SM parameters (M_Z , m_t , α_s and $\Delta\alpha_{\text{had}}^{(5)}(M_Z)$) are fixed to the best-fit values from that analysis. We emphasise that the study of the oblique parameters S, T, U is not sufficient, because the 2HDM involves Z vertex corrections [37–39]. For our analysis we have re-calculated the 2HDM contributions to the electroweak precision observables at one loop using the FeynArts, FormCalc and LoopTools packages [33–35]. The results have then been combined with the SM contributions (including all available higher-order corrections) using the prescription of Ref. [40]. The SM contributions to the EWPOs were calculated with the Zfitter software [41–43], with the exception of R_b , for which we use the improved results from [44].
- the branching ratio $\text{Br}(B \rightarrow X_s \gamma)$. We use the theoretical calculation of this quantity in the 2HDM in Refs. [45–50] and write [51]

$$\text{Br}(\bar{B} \rightarrow X_s \gamma)_{E > E_0} = \text{Br}(\bar{B} \rightarrow X_c e \bar{\nu})_{\text{exp}} \left| \frac{V_{ts}^* V_{tb}}{V_{cb}} \right|^2 \frac{6\alpha_{\text{em}}}{\pi \cdot C} [P(E_0) + N(E_0)] \quad , \quad (3.4)$$

where $E_0 = 1.6 \text{ GeV}$, $\text{Br}(\bar{B} \rightarrow X_c e \bar{\nu})_{\text{exp}} = 0.1072$ (Eq. 183 of [52]), $|V_{ts}^* V_{tb}/V_{cb}|^2 = 0.963$ (text before Eq. 1 of [53]) and $C = 0.546$ (Eq. 7 of [53]). The dependence on the 2HDM parameters is contained in the quantity $[P(E_0) + N(E_0)]$. To evaluate it we use private code provided by the authors of [50]. Following the discussion of theoretical errors in [50] we obtain a statistical error of 3% from the uncertainties of the parameters $\text{Br}(\bar{B} \rightarrow X_c e \bar{\nu})_{\text{exp}}$, $|V_{ts}^* V_{tb}/V_{cb}|^2$ and C and an overall systematic error of 12% (all other errors from [53] added linearly). In our fit, all these theoretical

errors are reflected by a single multiplicative nuisance parameter. Our experimental input for $\text{Br}(\bar{B} \rightarrow X_s \gamma)_{E > E_0}$ is [50]

$$\text{Br}(\bar{B} \rightarrow X_s \gamma)_{E > E_0}^{\text{exp}} = (3.37 \pm 0.23) \times 10^{-4} \quad . \quad (3.5)$$

- the mass splitting Δm_{B_s} in the neutral B_s meson system. For the theoretical computation of this quantity we use the expressions given in [12, 54–56]:

$$\Delta m_{B_s} = \frac{G_F^2}{24\pi^2} |V_{ts} V_{tb}^*|^2 \eta_B m_{B_s} \bar{m}_t^2 f_{B_s}^2 \hat{B}_{B_s} (S_{WW} + S_{WH} + S_{HH}) \quad , \quad (3.6)$$

where G_F is the Fermi constant and the dependence on the 2HDM parameters is in the quantities S_{WW} , S_{WH} and S_{HH} (see [12] for their definition). The values of the other pre-factors are

$$\begin{aligned} |V_{ts} V_{tb}^*|^2 &= 0.039986 && [57] \\ \eta_B &= 0.551 \pm 0.0022 \text{ (syst.)} && [12, 58] \\ m_{B_s} &= 5.3663 \text{ GeV} && [59] \\ \bar{m}_t &= 166.6 \text{ GeV} \quad \overline{MS} \text{ scheme} \\ f_{B_s} &= [0.229 \pm 0.002 \text{ (stat.)} \pm 0.006 \text{ (syst.)}] \text{ GeV} && [60] \\ \hat{B}_{B_s} &= 1.322 \pm 0.026 \text{ (stat.)} \pm 0.035 \text{ (syst.)} && [57, 61] \end{aligned}$$

By adding the statistical errors in quadrature and the systematic errors linearly we obtain a relative statistical uncertainty of 2.6% and a relative systematic uncertainty of ${}_{-8.5}^{+8.0}\%$. In our fit, these theoretical uncertainties are represented by a single multiplicative nuisance parameter. Our experimental input for Δm_{B_s} is [62]

$$\Delta m_{B_s} = [17.768 \pm 0.023 \text{ (stat.)} \pm 0.006 \text{ (syst.)}] \text{ (ps)}^{-1} \quad . \quad (3.7)$$

Let us briefly comment on our selection of flavour observables. In the type-II model under consideration, flavour-changing neutral current (FCNC) processes are sensitive to 2HDM effects for small and very large values of $\tan \beta$: if $\tan \beta < 1$, the charged-Higgs coupling to the top quark is enhanced. Conversely, for $\tan \beta \gtrsim 40$ the couplings of H , A , H^\pm to bottom quarks and tau leptons is of order 1, leading to sizable effects in (semi-)tauonic B decays [63–75] and $\text{Br}(B \rightarrow \ell^+ \ell^-)$ [76]. $\text{Br}(B \rightarrow X_s \gamma)$ plays a special role, because it provides a powerful lower bound on M_{H^\pm} which is essentially independent of $\tan \beta$, unless $\tan \beta < 1$ [45–50]. An early combined analysis of several flavour observables for $\tan \beta \leq 1$ can be found in Ref. [56]. An exhaustive analysis of several leptonic and semileptonic meson (and τ) decays, B - \bar{B} mixing, $\text{Br}(B \rightarrow X_s \gamma)$, and $Z \rightarrow b\bar{b}$ is presented in Ref. [12]. In the present paper we are interested in the low $\tan \beta$ region where the Higgs signal strengths still allow large deviations of α from the SM-like limit $\beta - \pi/2$. Therefore the only flavour observables relevant to our fit are $\text{Br}(B \rightarrow X_s \gamma)$ and the mass splitting Δm_{B_s} in the neutral B_s meson system. The ratio $\Delta m_B / \Delta m_{B_s}$ assumes the same value as in the SM. Therefore we do not need to include the weaker constraint from Δm_B in our fit. Furthermore, the

value of $|V_{ts}V_{tb}|$ governing both $\text{Br}(\bar{B} \rightarrow X_s\gamma)$ and Δm_{B_s} is not changed if one passes from the SM to the 2HDM: V_{tb} is approximately 1, V_{ts} is obtained from V_{cb} through CKM unitarity and the extra 2HDM Higgs bosons have no impact on the determination of V_{cb} . The omission of data on (semi-) tauonic B decays affects the fit only for large values of $\tan\beta$. Furthermore, the 2HDM of type II does not alleviate the tensions between the SM and the experimental world averages of $\text{Br}(B \rightarrow \tau\nu)$ and $\text{Br}(B \rightarrow D^{(*)}\tau\nu)$, but rather worsens the agreement with the data. (For an analysis of these decay modes in a general 2HDM see Ref. [77].)

4 Results

In this section we present the results of a global fit incorporating the constraints discussed in the last section. All fits were done with the *myFitter* framework [78] and cross-checked with an independent implementation in the CKMfitter software [79]. All p -values (and the corresponding 1σ , 2σ and 3σ exclusion limits) were computed by applying Wilks' theorem. Although this is common practice for analyses like the one presented here, it is not clear how reliable these p -values are as the presence of theoretical constraints violates the underlying assumptions of Wilks' theorem (see [78] for a discussion). For the present paper, we decided to follow standard practice and postpone further studies of this issue to a future publication.

Fig. 1(a) shows the regions in the $\tan\beta$ - $(\beta - \alpha)$ plane allowed at one, two and three standard deviations. Here and in the following plots, the shaded blue areas show the results of the fit with the tight perturbativity limit $\lambda_{\max} = 2\pi$. To gauge the sensitivity of the visible features on the implementation of the perturbativity bound the contours of the corresponding areas for the fit with $\lambda_{\max} = 4\pi$ are shown as green lines. The line with $\beta - \alpha = \pi/2$ corresponds to the case where the couplings of the light CP -even Higgs boson are the same as those of the SM Higgs boson. The best agreement with the experimental data is found along this line, which just reflects the fact that all the included experimental data is in good agreement with the predictions of the SM. For $\tan\beta < 0.6$ the value of $\beta - \alpha$ can not deviate from $\pi/2$ by more than 0.01π . This is a combined effect of the flavour, EWPO and perturbativity constraints. For small $\tan\beta$ the observables $\text{Br}(\bar{B} \rightarrow X_s\gamma)$, Δm_{B_s} and R_b receive large corrections from charged Higgs diagrams and thus force m_{H^\pm} to large values. In this limit the perturbativity bounds force α to be close to $\beta - \pi/2$. For $\tan\beta > 5$ there is a thin strip allowed at two standard deviations, where $\beta - \alpha$ can be as low as 0.4π . The best-fit scenarios in this strip feature relatively small masses of the heavy Higgs bosons (m_H between 400 GeV and 500 GeV), an enhanced hgg coupling and reduced hZZ , hWW and $h\gamma\gamma$ (effective) couplings.

Fig. 1(b) shows the allowed regions in the $\tan\beta$ - m_{H^\pm} plane. The exclusions in this plot are essentially due to the flavour observables $\text{Br}(\bar{B} \rightarrow X_s\gamma)$ and Δm_{B_s} as well as the hadronic $Z \rightarrow b\bar{b}$ branching ratio R_b . All these observables get contributions from charged Higgs diagrams which are proportional to positive powers of $\cot\beta$. Suppressing these terms for small values of $\tan\beta$ requires very large values of m_{H^\pm} , so that charged Higgs masses below 1 TeV are excluded for $\tan\beta \lesssim 0.8$. The β -independent terms in $\text{Br}(\bar{B} \rightarrow X_s\gamma)$

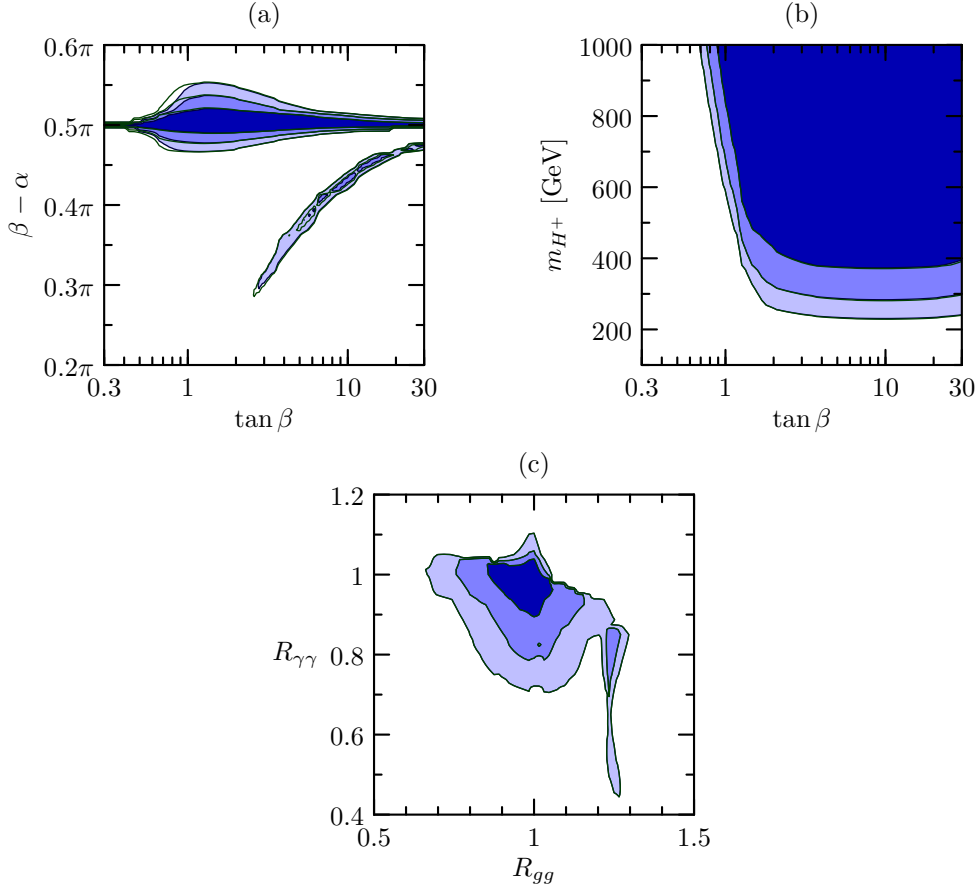


Figure 1: Allowed regions in the $\tan\beta$ - $(\beta - \alpha)$ plane (a), the $\tan\beta$ - m_{H^\pm} plane (b) and the R_{gg} - $R_{\gamma\gamma}$ plane (c). The shaded blue areas are the regions allowed at one, two and three standard deviations (dark to light) for the tight perturbativity constraint ($\lambda_{\max} = 2\pi$). The contours of the corresponding regions for $\lambda_{\max} = 4\pi$ are indicated by green lines.

lead to an absolute lower limit of 322 GeV at two standard deviations and approximately 400 GeV at one standard deviation. This limit is the main reason for the fact that the lower strip in Fig. 1(a) is disfavoured at one standard deviation. If we remove the flavour observables and R_b from our fit we confirm the results of previous analyses (e.g. [20, 21]) where the lower strip in Fig. 1(a) is still allowed at one standard deviation. Also note that the green lines in Fig. 1(b) exactly coincide with the boundaries of the blue regions, which means that the limits shown in this plot are insensitive to the implementation of the perturbativity bound. The pattern of Fig. 1(b) is the same as the one found in [12], but of course the newer data and the NNLO result used by us lead to a tighter lower bound on m_{H^\pm} .

Limits for the tree-level couplings of h to fermions, W and Z bosons can easily be extracted from Fig. 1(a) and Tab. 1. The relations between the 2HDM parameters and the one-loop effective hgg and $h\gamma\gamma$ couplings are more complicated. Fig. 1(c) shows exclusion limits in the R_{gg} - $R_{\gamma\gamma}$ plane, where R_{gg} and $R_{\gamma\gamma}$ are the (2HDM/SM) ratios of squared effective hgg and $h\gamma\gamma$ couplings, respectively. We see that the favoured region is centred

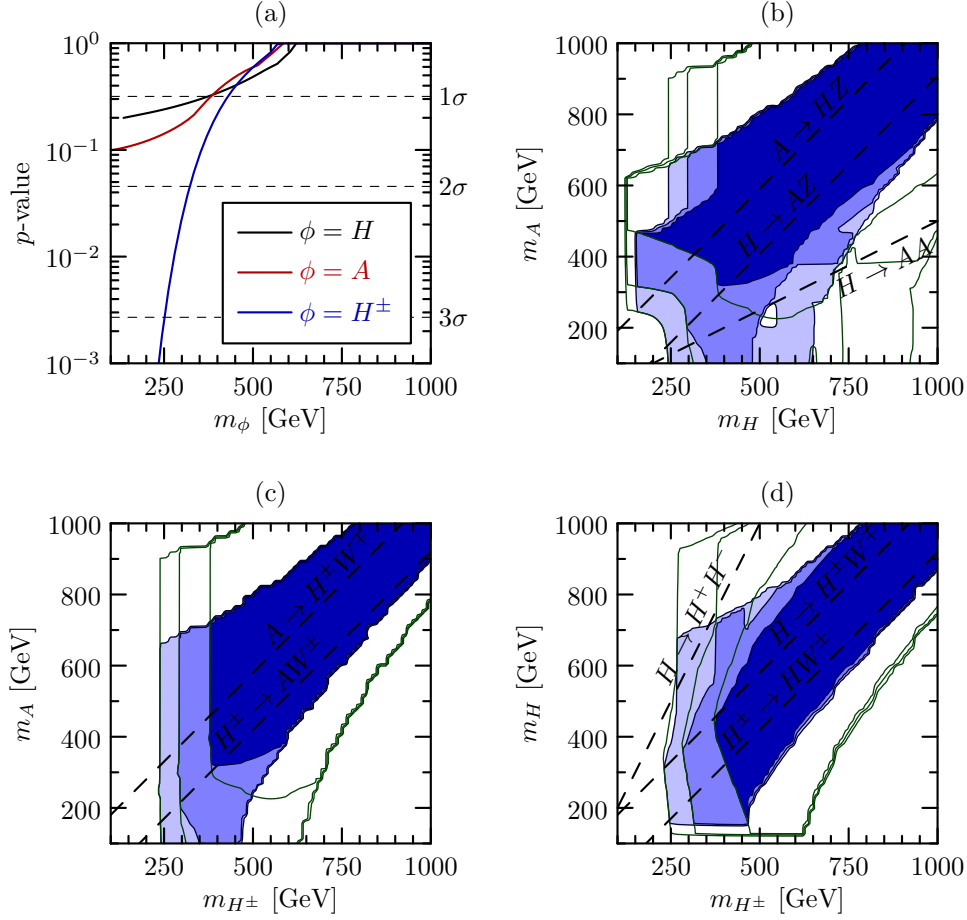


Figure 2: (a) shows p -values for the masses of the heavy 2HDM Higgs bosons. (b) to (d) shows allowed regions in the m_H - m_A , m_{H^\pm} - m_A and m_{H^\pm} - m_H planes, respectively. The shaded blue areas are the regions allowed at one, two and three standard deviations (dark to light) for the tight perturbativity constraint ($\lambda_{\max} = 2\pi$). The contours of the corresponding regions for $\lambda_{\max} = 4\pi$ are indicated by green lines. The dashed lines indicate thresholds for on-shell decays of one heavy 2HDM Higgs boson into other heavy 2HDM Higgs bosons.

around $R_{gg} = R_{\gamma\gamma} = 1$, i.e. the SM limit. In addition, there is a region around $R_{gg} = 1.25$ and $R_{\gamma\gamma} = 0.8$ which is allowed at two standard deviations. This region directly corresponds to the lower strip in Fig. 1(a).

The implications of the current experimental data for the masses of the heavy 2HDM Higgs bosons are summarised in Fig. 2. Fig. 2(a) shows, as a function of m_ϕ , the p -value for the hypothesis that a certain heavy 2HDM Higgs boson ϕ ($= H, A, H^\pm$) has a certain mass m_ϕ . In addition to the lower limits on m_{H^\pm} which were already shown in Fig. 1(b) we see that masses of the heavy neutral Higgs bosons below approximately 375 GeV are disfavoured at one standard deviation. At two standard deviations all values down to 126 GeV (in the case of m_H) or below (in the case of m_A) are allowed. However, certain combinations of heavy Higgs masses can be excluded with a higher significance. This is shown in Figs. 2(b) to (d). The dashed lines indicate the thresholds for various

tree-level $\phi \rightarrow \phi' \phi''$ and $\phi \rightarrow \phi' V$ decays (with $\phi, \phi', \phi'' \in \{H, A, H^\pm\}$ and $V \in \{W, Z\}$). Fig. 2(b) shows that scenarios where both m_H and m_A are smaller than 300 GeV are excluded at two standard deviations. In Fig. 2(d) we see that the lower limit of m_{H^\pm} increases slightly for values of m_H below approximately 400 GeV. These limits are due to the flavour and electroweak precision observables and independent of the implementation of the perturbativity bound. Furthermore, the top-left and bottom-right regions in Figs. 2(b) to (d) are excluded because the requirement of perturbativity constrains the differences between the heavy Higgs masses to be of order v . Naturally, these limits depend on the implementation of the perturbativity bound. For the tight bound ($\lambda_{\max} = 2\pi$) the (on-shell) decay $H \rightarrow H^+ H^-$ is excluded at two standard deviations.

5 Conclusions

In this paper we have confronted the type-II 2HDM (with a softly broken Z_2 symmetry) with the relevant experimental constraints from LHC data on the 126 GeV Higgs resonance, the non-observation of additional heavy Higgs resonances, electroweak precision and flavour observables. In addition theoretical constraints from the requirements of vacuum stability and perturbativity were taken into account. While the requirement for perturbativity of the Higgs self-couplings must be included in some way, we emphasise that the definition of the perturbativity bound involves some arbitrariness. Therefore, the approach taken in this paper is to show results for both a loose ($\lambda_{\max} = 4\pi$) and a tight ($\lambda_{\max} = 2\pi$) implementation of this bound.

In the present analysis the 126 GeV resonance is always interpreted as the light CP -even 2HDM Higgs boson. We find that the combination of Higgs signal strength data and flavour observables disfavour, at one standard deviation, scenarios where the couplings of light CP -even Higgs boson deviate strongly from the ones of the SM Higgs boson. (We are referring to the 2σ ‘islands’ in Fig. 1(a) and (c).) For $\tan \beta < 5$ such scenarios are excluded at two standard deviations. Charged Higgs masses below 322 GeV are also excluded at two standard deviations. This limit is mainly due to the $\text{Br}(\bar{B} \rightarrow X_s \gamma)$ measurement and our fit uses the most accurate available theoretical computation [50, 51] of this quantity. Furthermore, flavour and electroweak precision observables exclude scenarios with both m_H and m_A below approximately 300 GeV at two standard deviations. For large values of m_H , m_A and m_{H^\pm} the differences between these masses are bounded by the requirement of perturbativity. If the tight version ($\lambda_{\max} = 2\pi$) of the perturbativity bound is employed, the on-shell $H \rightarrow H^+ H^-$ decay is ruled out at two standard deviations.

Our results differ with several recent analyses of the 2HDM of type II. Contrary to statements in e.g. [20, 21] we find that scenarios where $\beta - \alpha$ deviates significantly from $\pi/2$ are disfavoured at one standard deviation and excluded at two standard deviations for $\tan \beta < 5$. This exclusion is a consequence of the combination of light Higgs signal strengths with flavour observables. We also do not confirm the upper limits on the heavy Higgs masses reported in [22]. As explained in [23] the type-II 2HDM with a softly broken Z_2 symmetry has a decoupling limit in which the light CP -even Higgs boson becomes SM-like and the other Higgs bosons become infinitely heavy. In this limit the theory is phenomenologi-

cally indistinguishable from the SM and perturbativity of the Higgs self-couplings enforces precise relations between the heavy Higgs masses. The scan-based analysis of [22] simply misses the scenarios where these relations are fulfilled. For the same reason, we do not confirm the upper limit on $\tan\beta$ reported there.

Acknowledgements

We would like to thank Thomas Hermann, Mikolaj Misiak and Matthias Steinhauser for sharing their code for $\text{Br}(\bar{B} \rightarrow X_s \gamma)$ with us. We also thank the CKMfitter group for access to and support for their analysis framework.

References

- [1] CMS Collaboration, S. Chatrchyan et al., *Observation of a new boson at a mass of 125 GeV with the CMS experiment at the LHC*, Phys.Lett. **B716** (2012) 30–61, [[arXiv:1207.7235](#)].
- [2] ATLAS Collaboration, G. Aad et al., *Observation of a new particle in the search for the Standard Model Higgs boson with the ATLAS detector at the LHC*, Phys.Lett. **B716** (2012) 1–29, [[arXiv:1207.7214](#)].
- [3] A. Djouadi and A. Lenz, *Sealing the fate of a fourth generation of fermions*, Phys.Lett. **B715** (2012) 310–314, [[arXiv:1204.1252](#)].
- [4] E. Kuflik, Y. Nir, and T. Volansky, *Implications of Higgs Searches on the Four Generation Standard Model*, [arXiv:1204.1975](#).
- [5] O. Eberhardt, G. Herbert, H. Lacker, A. Lenz, A. Menzel, U. Nierste, and M. Wiebusch, *Joint analysis of Higgs decays and electroweak precision observables in the Standard Model with a sequential fourth generation*, Phys.Rev. **D86** (2012) 013011, [[arXiv:1204.3872](#)].
- [6] M. Buchkremer, J.-M. Gerard, and F. Maltoni, *Closing in on a perturbative fourth generation*, JHEP **1206** (2012) 135, [[arXiv:1204.5403](#)].
- [7] O. Eberhardt, A. Lenz, A. Menzel, U. Nierste, and M. Wiebusch, *Status of the fourth fermion generation before ICHEP2012: Higgs data and electroweak precision observables*, [arXiv:1207.0438](#).
- [8] O. Eberhardt, G. Herbert, H. Lacker, A. Lenz, A. Menzel, U. Nierste, and M. Wiebusch, *Impact of a Higgs boson at a mass of 126 GeV on the standard model with three and four fermion generations*, Phys.Rev.Lett. **109** (2012) 241802, [[arXiv:1209.1101](#)].
- [9] T. Lee, *A Theory of Spontaneous T Violation*, Phys.Rev. **D8** (1973) 1226–1239.
- [10] S. L. Glashow and S. Weinberg, *Natural Conservation Laws for Neutral Currents*, Phys.Rev. **D15** (1977) 1958.
- [11] J. F. Donoghue and L. F. Li, *Properties of Charged Higgs Bosons*, Phys.Rev. **D19** (1979) 945.
- [12] O. Deschamps, S. Descotes-Genon, S. Monteil, V. Niess, S. T’Jampens, et al., *The Two Higgs Doublet of Type II facing flavour physics data*, Phys.Rev. **D82** (2010) 073012, [[arXiv:0907.5135](#)].
- [13] D. Carmi, A. Falkowski, E. Kuflik, T. Volansky, and J. Zupan, *Higgs After the Discovery: A Status Report*, [arXiv:1207.1718](#).

- [14] H. Cheon and S. K. Kang, *Constraining parameter space in type-II two-Higgs doublet model in light of a 125 GeV Higgs boson*, [arXiv:1207.1083](#).
- [15] A. Drozd, B. Grzadkowski, J. F. Gunion, and Y. Jiang, *Two-Higgs-Doublet Models and Enhanced Rates for a 125 GeV Higgs*, [arXiv:1211.3580](#).
- [16] P. Ferreira, R. Santos, M. Sher, and J. P. Silva, *Implications of the LHC two-photon signal for two-Higgs-doublet models*, [arXiv:1112.3277](#).
- [17] C.-Y. Chen and S. Dawson, *Exploring Two Higgs Doublet Models Through Higgs Production*, [arXiv:1301.0309](#).
- [18] A. Celis, V. Ilisie, and A. Pich, *LHC constraints on two-Higgs doublet models*, [arXiv:1302.4022](#).
- [19] P. P. Giardino, K. Kannike, I. Masina, M. Raidal, and A. Strumia, *The universal Higgs fit*, [arXiv:1303.3570](#).
- [20] B. Grinstein and P. Uttayarat, *Carving Out Parameter Space in Type-II Two Higgs Doublets Model*, [arXiv:1304.0028](#).
- [21] A. Barroso, P. Ferreira, R. Santos, M. Sher, and J. P. Silva, *2HDM at the LHC - the story so far*, [arXiv:1304.5225](#).
- [22] B. Coleppa, F. Kling, and S. Su, *Constraining Type II 2HDM in Light of LHC Higgs Searches*, [arXiv:1305.0002](#).
- [23] J. F. Gunion and H. E. Haber, *The CP conserving two Higgs doublet model: The Approach to the decoupling limit*, Phys.Rev. **D67** (2003) 075019, [[hep-ph/0207010](#)].
- [24] A. Barroso, P. Ferreira, I. Ivanov, and R. Santos, *Metastability bounds on the two Higgs doublet model*, [arXiv:1303.5098](#).
- [25] U. Nierste and K. Riesselmann, *Higgs sector renormalization group in the \overline{MS} and \overline{OMS} scheme: The Breakdown of perturbation theory for a heavy Higgs*, Phys.Rev. **D53** (1996) 6638–6652, [[hep-ph/9511407](#)].
- [26] ATLAS conference note, ATLAS-CONF-2013-012.
- [27] ATLAS conference note, ATLAS-CONF-2013-013.
- [28] CMS physics analysis summary, CMS-PAS-HIG-13-001.
- [29] CMS physics analysis summary, CMS-PAS-HIG-13-002.
- [30] P. Ferreira, R. Santos, M. Sher, and J. P. Silva, *Could the LHC two-photon signal correspond to the heavier scalar in two-Higgs-doublet models?*, Phys.Rev. **D85** (2012) 035020, [[arXiv:1201.0019](#)].
- [31] G. Burdman, C. E. Haluch, and R. D. Matheus, *Is the LHC Observing the Pseudo-scalar State of a Two-Higgs Doublet Model ?*, Phys.Rev. **D85** (2012) 095016, [[arXiv:1112.3961](#)].
- [32] P. Ferreira, H. E. Haber, R. Santos, and J. P. Silva, *Mass-degenerate Higgs bosons at 125 GeV in the Two-Higgs-Doublet Model*, [arXiv:1211.3131](#).
- [33] T. Hahn and M. Perez-Victoria, *Automatized one-loop calculations in four and D dimensions*, Comput. Phys. Commun. **118** (1999) 153–165, [[hep-ph/9807565](#)].
- [34] T. Hahn, *Generating Feynman diagrams and amplitudes with FeynArts 3*, Comput. Phys. Commun. **140** (2001) 418–431, [[hep-ph/0012260](#)].

- [35] T. Hahn and M. Rauch, *News from FormCalc and LoopTools*, Nucl. Phys. Proc. Suppl. **157** (2006) 236–240, [[hep-ph/0601248](#)].
- [36] CMS physics analysis summary, CMS-PAS-HIG-13-003.
- [37] W. Hollik, *Nonstandard Higgs bosons in $SU(2) \times U(1)$ radiative corrections*, Z.Phys. **C32** (1986) 291.
- [38] W. Hollik, *Radiative corrections with two Higgs doublets at LEP/SLC and HERA*, Z.Phys. **C37** (1988) 569.
- [39] H. E. Haber and H. E. Logan, *Radiative corrections to the $Z b$ anti- b vertex and constraints on extended Higgs sectors*, Phys.Rev. **D62** (2000) 015011, [[hep-ph/9909335](#)].
- [40] P. Gonzalez, J. Rohrwild, and M. Wiebusch, *Electroweak Precision Observables within a Fourth Generation Model with General Flavour Structure*, Eur.Phys.J. **C72** (2012) 2007, [[arXiv:1105.3434](#)].
- [41] D. Y. Bardin, M. S. Bilenky, T. Riemann, M. Sachwitz, and H. Vogt, *DIZET: A Program Package for the Calculation of Electroweak One Loop Corrections for the Process $e^+e^- \rightarrow f^+f^-$ Around the Z^0 Peak*, Comput.Phys.Commun. **59** (1990) 303–312.
- [42] D. Y. Bardin, P. Christova, M. Jack, L. Kalinovskaya, A. Olchevski, et al., *ZFITTER v.6.21: A Semianalytical program for fermion pair production in e^+e^- annihilation*, Comput.Phys.Commun. **133** (2001) 229–395, [[hep-ph/9908433](#)].
- [43] A. Arbuzov, M. Awramik, M. Czakon, A. Freitas, M. Grunewald, et al., *ZFITTER: A Semi-analytical program for fermion pair production in e^+e^- annihilation, from version 6.21 to version 6.42*, Comput.Phys.Commun. **174** (2006) 728–758, [[hep-ph/0507146](#)].
- [44] A. Freitas and Y.-C. Huang, *Electroweak two-loop corrections to $\sin^2\theta_{\text{eff},bb}$ and R_b using numerical Mellin-Barnes integrals*, JHEP **1208** (2012) 050, [[arXiv:1205.0299](#)].
- [45] M. Ciuchini, G. Degrossi, P. Gambino, and G. Giudice, *Next-to-leading QCD corrections to $B \rightarrow X_s\gamma$: Standard model and two Higgs doublet model*, Nucl.Phys. **B527** (1998) 21–43, [[hep-ph/9710335](#)].
- [46] F. Borzumati and C. Greub, *2HDMs predictions for $\bar{B} \rightarrow X_s\gamma$ in NLO QCD*, Phys.Rev. **D58** (1998) 074004, [[hep-ph/9802391](#)].
- [47] F. Borzumati and C. Greub, *Two Higgs doublet model predictions for $\bar{B} \rightarrow X_s\gamma$ in NLO QCD: Addendum*, Phys.Rev. **D59** (1999) 057501, [[hep-ph/9809438](#)].
- [48] P. Ciafaloni, A. Romanino, and A. Strumia, *Two loop QCD corrections to charged Higgs mediated $b \rightarrow s\gamma$ decay*, Nucl.Phys. **B524** (1998) 361–376, [[hep-ph/9710312](#)].
- [49] C. Bobeth, M. Misiak, and J. Urban, *Matching conditions for $b \rightarrow s\gamma$ and $b \rightarrow sg$ in extensions of the standard model*, Nucl.Phys. **B567** (2000) 153–185, [[hep-ph/9904413](#)].
- [50] T. Hermann, M. Misiak, and M. Steinhauser, *$\bar{B} \rightarrow X_s\gamma$ in the Two Higgs Doublet Model up to Next-to-Next-to-Leading Order in QCD*, JHEP **1211** (2012) 036, [[arXiv:1208.2788](#)].
- [51] M. Misiak and M. Steinhauser, *NNLO QCD corrections to the $\bar{B} \rightarrow X_s\gamma$ matrix elements using interpolation in m_c* , Nucl.Phys. **B764** (2007) 62–82, [[hep-ph/0609241](#)].
- [52] **Heavy Flavor Averaging Group**, Y. Amhis et al., *Averages of B-Hadron, C-Hadron, and tau-lepton properties as of early 2012*, [arXiv:1207.1158](#).
- [53] P. Gambino and P. Giordano, *Normalizing inclusive rare B decays*, Phys.Lett. **B669** (2008) 69–73, [[arXiv:0805.0271](#)].

- [54] L. Abbott, P. Sikivie, and M. B. Wise, *Constraints on Charged Higgs Couplings*, Phys.Rev. **D21** (1980) 1393.
- [55] C. Geng and J. N. Ng, *CHARGED HIGGS EFFECT IN $B(d)0$ - anti- $B(d)0$ MIXING, $K \rightarrow \pi$ neutrino anti-neutrino DECAY AND RARE DECAYS OF B MESONS*, Phys.Rev. **D38** (1988) 2857.
- [56] A. J. Buras, P. Krawczyk, M. E. Lautenbacher, and C. Salazar, *B^0 - \bar{B}^0 mixing, CP violation, $K^+ \rightarrow \pi^+ \nu \bar{\nu}$ and $B \rightarrow K \gamma X$ in a two Higgs doublet model*, Nucl.Phys. **B337** (1990) 284–312.
- [57] Private communication with the CKMfitter group.
- [58] A. J. Buras, M. Jamin, and P. H. Weisz, *Leading and next-to-leading QCD corrections to ε parameter and B^0 - \bar{B}^0 mixing in the presence of a heavy top quark*, Nucl.Phys. **B347** (1990) 491–536.
- [59] **Particle Data Group**, J. Beringer et al., *Review of Particle Physics (RPP)*, Phys.Rev. **D86** (2012) 010001.
- [60] A. Lenz, U. Nierste, J. Charles, S. Descotes-Genon, H. Lacker, et al., *Constraints on new physics in $B - \bar{B}$ mixing in the light of recent LHCb data*, Phys.Rev. **D86** (2012) 033008, [[arXiv:1203.0238](#)].
- [61] **HPQCD** Collaboration, E. Gamiz, C. T. Davies, G. P. Lepage, J. Shigemitsu, and M. Wingate, *Neutral B Meson Mixing in Unquenched Lattice QCD*, Phys.Rev. **D80** (2009) 014503, [[arXiv:0902.1815](#)].
- [62] **LHCb**, R. Aaij et al., *Precision measurement of the $B_s^0 - \bar{B}_s^0$ oscillation frequency with the decay $B_s^0 \rightarrow D_s^- \pi^+$* , [arXiv:1304.4741](#).
- [63] W.-S. Hou, *Enhanced charged Higgs boson effects in B^- to tau anti-neutrino, mu anti-neutrino and b to tau anti-neutrino + X* , Phys.Rev. **D48** (1993) 2342–2344.
- [64] A. Akeroyd and S. Recksiegel, *The Effect of H^{\pm} on $B^{\pm} \rightarrow \tau \nu$ and $B^{\pm} \rightarrow \mu \nu$ muon neutrino*, J.Phys. **G29** (2003) 2311–2317, [[hep-ph/0306037](#)].
- [65] B. Grzadkowski and W.-S. Hou, *Searching for $B \rightarrow D \tau \bar{\nu}$ neutrino at the 10-percent level*, Phys.Lett. **B283** (1992) 427–433.
- [66] T. Miki, T. Miura, and M. Tanaka, *Effects of charged Higgs boson and QCD corrections in anti- $B \rightarrow D$ tau anti- $\nu(\tau)$* , [hep-ph/0210051](#).
- [67] U. Nierste, S. Trine, and S. Westhoff, *Charged-Higgs effects in a new $B \rightarrow D$ tau nu differential decay distribution*, Phys.Rev. **D78** (2008) 015006, [[arXiv:0801.4938](#)].
- [68] J. F. Kamenik and F. Mescia, *$B \rightarrow D$ tau nu Branching Ratios: Opportunity for Lattice QCD and Hadron Colliders*, Phys.Rev. **D78** (2008) 014003, [[arXiv:0802.3790](#)].
- [69] S. Trine, *Charged-Higgs effects in $B \rightarrow (D)$ tau nu decays*, [arXiv:0810.3633](#).
- [70] M. Tanaka and R. Watanabe, *Tau longitudinal polarization in $B \rightarrow D$ tau nu and its role in the search for charged Higgs boson*, Phys.Rev. **D82** (2010) 034027, [[arXiv:1005.4306](#)].
- [71] S. Fajfer, J. F. Kamenik, and I. Nisandzic, *On the $B \rightarrow D^* \tau \bar{\nu}_\tau$ Sensitivity to New Physics*, Phys.Rev. **D85** (2012) 094025, [[arXiv:1203.2654](#)].
- [72] Y. Sakaki and H. Tanaka, *Constraints of the Charged Scalar Effects Using the Forward-Backward Asymmetry on $B \rightarrow D^{(*)} \tau \bar{\nu}_\tau$* , Phys.Rev. **D87** (2013) 054002, [[arXiv:1205.4908](#)].

- [73] D. Becirevic, N. Kosnik, and A. Tayduganov, $\bar{B} \rightarrow D\tau\bar{\nu}_\tau$ vs. $\bar{B} \rightarrow D\mu\bar{\nu}_\mu$, Phys.Lett. **B716** (2012) 208–213, [[arXiv:1206.4977](#)].
- [74] A. Celis, M. Jung, X.-Q. Li, and A. Pich, *Sensitivity to charged scalars in $B \rightarrow D^{(*)}\tau\nu_\tau$ and $B \rightarrow \tau\nu_\tau$ decays*, JHEP **1301** (2013) 054, [[arXiv:1210.8443](#)].
- [75] M. Tanaka and R. Watanabe, *New physics in the weak interaction of $\bar{B} \rightarrow D^{(*)}\tau\bar{\nu}$* , Phys.Rev. **D87** (2013) 034028, [[arXiv:1212.1878](#)].
- [76] H. E. Logan and U. Nierste, $B_{s,d} \rightarrow \ell^+\ell^-$ in a two Higgs doublet model, Nucl.Phys. **B586** (2000) 39–55, [[hep-ph/0004139](#)].
- [77] A. Crivellin, C. Greub, and A. Kokulu, *Explaining $B \rightarrow D\tau\nu$, $B \rightarrow D^*\tau\nu$ and $B \rightarrow \tau\nu$ in a 2HDM of type III*, Phys.Rev. **D86** (2012) 054014, [[arXiv:1206.2634](#)].
- [78] M. Wiebusch, *Numerical Computation of p-values with myFitter*, [[arXiv:1207.1446](#)].
- [79] A. Hocker, H. Lacker, S. Laplace, and F. Le Diberder, *A New approach to a global fit of the CKM matrix*, Eur.Phys.J. **C21** (2001) 225–259, [[hep-ph/0104062](#)].
- [80] CMS physics analysis summary, CMS-PAS-HIG-12-043.
- [81] ATLAS conference note, ATLAS-CONF-2012-091, Table 6.
- [82] **CDF, D0** Collaborations, *Higgs Boson Studies at the Tevatron*, [[arXiv:1303.6346](#)].
- [83] **ATLAS** Collaboration, G. Aad et al., *Combined search for the Standard Model Higgs boson in pp collisions at $\sqrt{s} = 7$ TeV with the ATLAS detector*, Phys.Rev. **D86** (2012) 032003, [[arXiv:1207.0319](#)].
- [84] ATLAS conference note, ATLAS-CONF-2012-091, Fig. 14a.
- [85] ATLAS conference note, ATLAS-CONF-2013-030.
- [86] ATLAS conference note, ATLAS-CONF-2012-161.
- [87] ATLAS conference note, ATLAS-CONF-2012-160.
- [88] CMS physics analysis summary, CMS-PAS-HIG-12-020.
- [89] CMS physics analysis summary, CMS-PAS-HIG-12-045.
- [90] CMS physics analysis summary, CMS-PAS-HIG-13-004.

	ggF	VBF	VH
0/1 jet [%]	0.945	2.101	1.702
VBF [%]	0.026	0.979	0.023

Table 2: Selection efficiencies for the different Higgs production mechanisms in the $H \rightarrow \tau\tau$ event categories defined by CMS [80] (see also Fig. 3). The columns stand for gluon fusion (ggF), vector boson fusion (VBF) and WH or ZH associated production (VH).

		ggF	VBF	WH	ZH	ttH
ATLAS 7 TeV	ucl	0.929	0.040	0.018	0.010	0.002
	uch	0.665	0.157	0.099	0.057	0.024
	url	0.928	0.039	0.020	0.011	0.002
	urh	0.654	0.161	0.108	0.061	0.018
	ccl	0.928	0.040	0.019	0.010	0.002
	cch	0.666	0.153	0.100	0.057	0.025
	crl	0.928	0.038	0.020	0.011	0.002
	crh	0.653	0.160	0.110	0.059	0.018
	ct	0.894	0.052	0.033	0.017	0.003
	jj	0.225	0.767	0.004	0.002	0.001
ATLAS 8 TeV	ucl	0.937	0.040	0.014	0.008	0.002
	uch	0.793	0.126	0.041	0.025	0.014
	url	0.932	0.040	0.016	0.010	0.001
	urh	0.781	0.133	0.047	0.028	0.011
	ccl	0.936	0.040	0.013	0.009	0.002
	cch	0.789	0.126	0.043	0.027	0.015
	crl	0.932	0.041	0.016	0.010	0.001
	crh	0.777	0.130	0.052	0.030	0.011
	ct	0.907	0.055	0.022	0.013	0.002
	lhm2j	0.450	0.541	0.005	0.003	0.001
	thm2j	0.238	0.760	0.001	0.001	0.000
	lm2j	0.481	0.030	0.297	0.172	0.019
	etmiss	0.041	0.005	0.357	0.476	0.121
	lept	0.022	0.006	0.632	0.154	0.186
CMS 7 TeV	u0	0.614	0.168	0.121	0.066	0.031
	u1	0.876	0.062	0.036	0.020	0.005
	u2	0.913	0.044	0.025	0.014	0.003
	u3	0.913	0.044	0.026	0.015	0.002
	jj	0.268	0.725	0.004	0.002	0.000
	CMS 8 TeV	u0	0.729	0.116	0.082	0.047
u1		0.835	0.084	0.045	0.026	0.010
u2		0.916	0.045	0.023	0.013	0.004
u3		0.925	0.039	0.021	0.012	0.003
jj t		0.207	0.789	0.002	0.001	0.001
jj l		0.470	0.509	0.011	0.006	0.005
mu		0.000	0.002	0.504	0.286	0.208
e		0.011	0.004	0.502	0.285	0.198
Etmiss		0.220	0.026	0.407	0.230	0.117

Table 3: Fractional contributions of the different Higgs production mechanisms to the $H \rightarrow \gamma\gamma$ event categories defined by ATLAS and CMS. The numbers and category labels are from [26, 28, 81] (see also Fig. 3). The columns stand for gluon fusion (ggF), vector boson fusion (VBF), WH associated production (WH), ZH associated production (ZH) and $t\bar{t}H$ associated production (ttH).

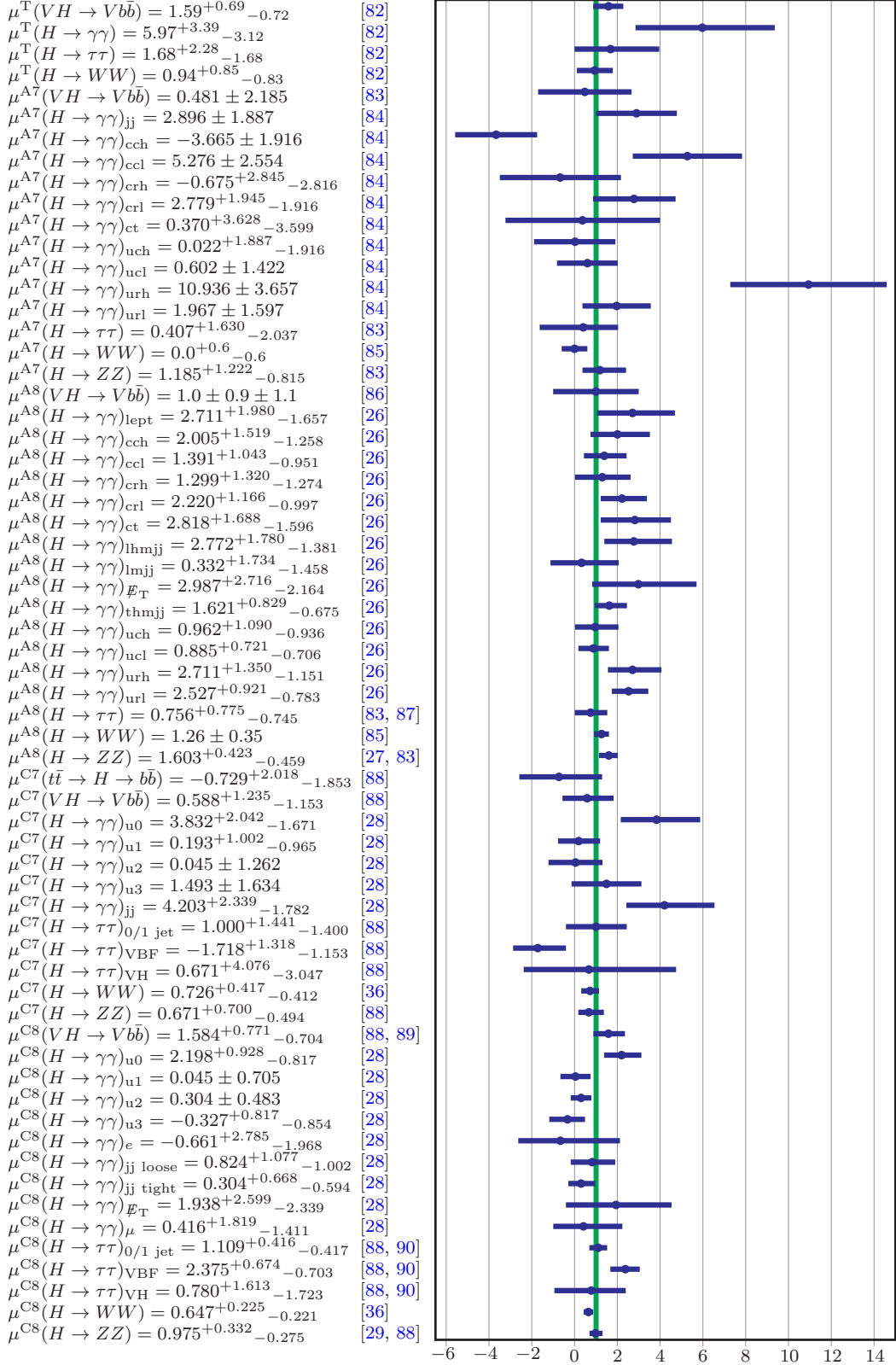


Figure 3: Higgs signal strengths measured by D0, CDF, ATLAS and CMS. The superscripts T, A7, A8, C7 and C8 refer to Tevatron, ATLAS 7 TeV, ATLAS 8 TeV, CMS 7 TeV and CMS 8 TeV data, respectively. The subscripts jj, cch etc. denote the different event categories defined by ATLAS and CMS. The combination of all signal strengths yields $\mu_{\text{combined}} = 1.007^{+0.099}_{-0.098}$ and is illustrated by the green band.